Available online at www.sciencedirect.com
SCIENCE DIRECT®
Journal of Nuclear Materials 343 (2005) 169–177
journal of nuclear materials
www.elsevier.com/locate/jnucmat

Thermal hydraulic design and decay heat removal of a solid target for a spallation neutron source

N. Takenaka [a,*], D. Nio [b], Y. Kiyanagi [b], K. Mishima [c], M. Kawai [d], M. Furusaka [d]

[a] Department of Mechanical Engineering, Kobe University, Kobe, Japan
[b] Hokkaido University, Sapporo, Japan
[c] Kyoto University Research Reactor Institute, Kumatori, Japan
[d] High Energy Accelerator Research Institute, Tsukuba, Japan

Abstract

Thermal hydraulic design and thermal stress calculations were conducted for a water-cooled solid target irradiated by a MW-class proton beam for a spallation neutron source. Plate type and rod bundle type targets were examined. The thickness of the plate and the diameter of the rod were determined based on the maximum and the wall surface temperature. The thermal stress distributions were calculated by a finite element method (FEM). The neutronics performance of the target is roughly proportional to its average density. The averaged densities of the designed targets were calculated for tungsten plates, tantalum–clad tungsten plates, tungsten rods sheathed by tantalum and Zircaloy and they were compared with mercury density. It was shown that the averaged density was highest for the tungsten plates and was high for the tantalum cladding tungsten plates, the tungsten rods sheathed by tantalum and Zircaloy in order. They were higher than or equal to that of mercury for the 1–2 MW proton beams. Tungsten target without the cladding or the sheath is not practical due to corrosion by water under irradiation condition. Therefore, the tantalum cladding tungsten plate already made successfully by HIP and the sheathed tungsten rod are the candidate of high performance solid targets. The decay heat of each target was calculated. It was low enough low compared to that of ISIS for the target without tantalum but was about four times as high as that of ISIS when the thickness of the tantalum cladding was 0.5 mm. Heat removal methods of the decay heat with tantalum were examined. It was shown that a special cooling system was required for the target exchange when tantalum was used for the target. It was concluded that the tungsten rod target sheathed with stainless steel or Zircaloy was the most reliable from the safety considerations and had similar neutronics performance to that of mercury.

1. Introduction

Water cooled solid targets of a high energy proton beam have been used for spallation neutron sources. A tantalum plate target has been irradiated by a 800 MeV and 2 mA pulsed proton beam in ISIS in

* Corresponding author. Tel./fax: +81 78 803 6118.
E-mail address: takenaka@mech.kobe-u.ac.jp (N. Takenaka).

0022-3115/$ - see front matter © 2005 Elsevier B.V. All rights reserved.
doi:10.1016/j.jnucmat.2004.11.017

Nomenclature

d	target plate thickness [m]	λ	thermal conductivity [W/m K]
d_w	diameter of wrapping wire for rod target [m]	ν	kinematic viscosity [m^2/s]
D	diameter of rod [m]	ρ	density [kg/m^3]
h	heat transfer coefficient [W/m^2 K]	σ	nominal stress [Pa]
L_{eff}	effective length of target for neutron production [m]	*Subscripts*	
Nu	Nusselt number	ch	coolant channel
Pr	Prandtl number	g	gas
q	heat flux [W/m^2]	in	inlet
Q	volumetric heat generation rate [W/m^3]	L	coolant
Re	Reynolds number	max	maximum
T	temperature [°C]	s	solid
u	water velocity [m/s]	VM	Von Mieses
W_p	proton beam power [MW]	w	target wall surface

Rutherford Appleton Laboratory. The beam power of 160 kW is the highest pulsed beam power for pulsed spallation neutron source in the world at present. Parallel 23 plates were placed and heavy water flows in 1.75 mm gaps between the plates. The minimum thickness of the target plate is 7.7 mm. The target has been exchanged without any special cooling after 1 week water flow cooling of decay heat from the beam off. The highest power continuous spallation neutron source is SINQ in Paul Sherrer Institute. A continuous proton beam of 570 MeV and 0.85 mA has been irradiated on a target made up from 450 Zircaloy-2 rods of 10.8 mm in diameter, arranged in a closely packed array with a pitch of 1.2 mm and cooled in a cross-flow configuration. After heat is low and no special attention has been reported for the decay heat removal by the target exchange.

Two high intense pulsed spallation neutron sources have been constructing in the projects of J-PARC (Japan Proton Accelerator Research Complex) and SNS (spallation neutron source) in USA. A MW-class proton beam will be irradiated to a mercury target. Solid targets for the MW-class beam were discussed in this paper. Thermal hydraulic and decay heat removal designs of the solid targets were carried out for the proton beam of J-PARC. Water cooled plate and rod targets as shown in Fig. 1 were examined. Tungsten and tantalum cladding tungsten plates and tungsten rods sheathed by tantalum, Zircaloy and stainless steel were used to the designs and the temperature and thermal stress distributions were calculated. The gap of the rod bundle can be fixed by spirally wrapping wires which have been used in sodium cooled fast breeder reactors. The averaged density of the designed target was discussed since the neutronics performance of the target is roughly proportional to its average density.

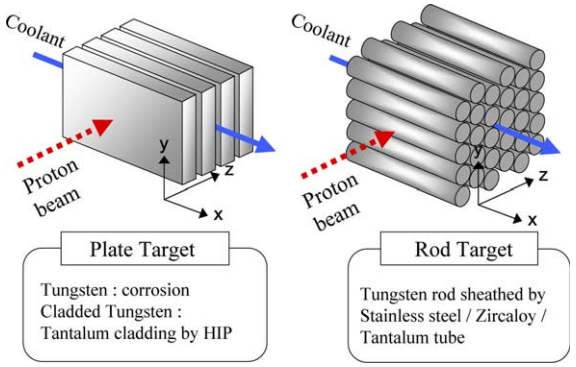

Fig. 1. Water cooled solid targets.

2. Thermal hydraulic design

Heat deposition rates of a proton beam irradiated to a pure tungsten target were calculated by a Monte-Carlo method by Kiyanagi and Furusaka [1]. The beam shape in cross-section was an ellipsoid of 40 mm and 140 mm in diameters and the intensity distribution was assumed to be parabolic. It was irradiated to a target block 60 mm × 166.7 mm in rectangular cross-section as shown in Fig. 2(a) and (b) and 500 mm in depth. The energy of the proton beam was 3 GeV. The calculated axial distributions of the volumetric heat deposition rates along the proton beam line were obtained and the values averaged in the whole cross-section (axis) are shown in Fig. 2(a) and averaged in a cylinder 20 mm in diameter at the center of the cross-section (center axis) in Fig. 2(b). The heat deposition rates are proportional to the beam power and those for the 1 MW proton beam are plotted against the target depth in Fig. 3. The both calculated results were fitted with empirical equations

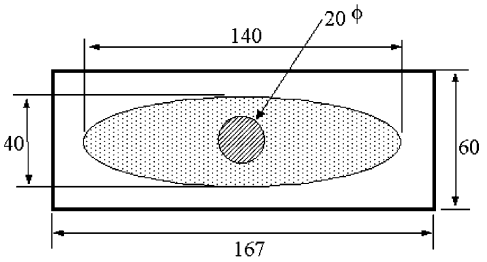

Fig. 2. Target plate and the proton beam shape.

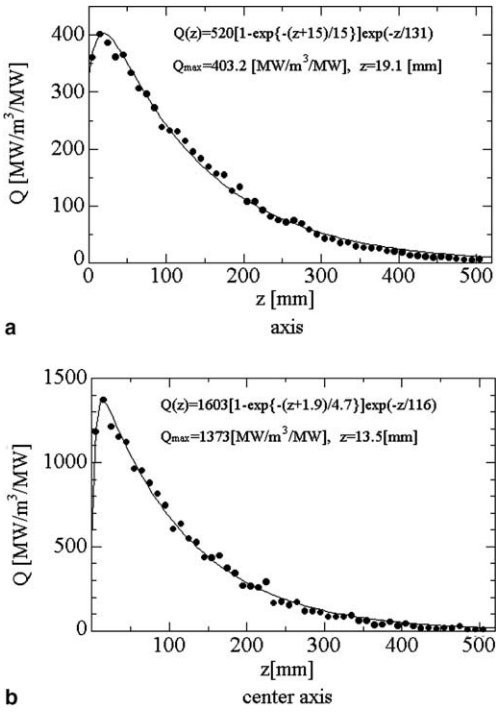

Fig. 3. (a) and (b) The axial volumetric heat deposition rates working for the target vessel calculated by a Monte-Carlo method for 3 GeV proton beam.

and are also shown in Fig. 3(a) and (b), respectively. The heat deposition rates have peaks near the beam window and decrease exponentially with increasing the target depth.

The target was sliced to make water flow channels in the plate target as shown in Fig. 1. All target plates were parallel for the targets in KENS. Two or three plates placed parallel were connected in series for that of ISIS. Since the pressure drop in the ISIS type flow channels was estimated to be too high for the flow velocity required to cool the high heat deposition rate for the MW-class beam, the target plate configuration like KENS was examined for the plate target. The distribution of the target plate thickness was designed based on the axial heat deposition rate distribution.

The cross-flow cools the target rods in SINQ. The axial flow as shown in Fig. 1 was employed to the present rod target design since the gap between the rods can be design more narrow to increase the averaged density. The diameter of the rods is fixed to make a bundle and is designed based on the heat deposition rate at the peak.

Boiling in the flow channel should be avoided since it may cause the flow instabilities and dryout in parallel channel. The averaged density of the target should be high for the neutron performance. The water irradiated by the proton beam should be minimized to increase the neutron production efficiency since the water is just void of the target for the neutron production and to decrease radioactive productions like ^{3}H and ^{7}Be generated by the nuclear spallation reactions of oxygen in the water.

The target wall surface and the maximum temperatures are highest at the center of the target. To estimate the highest temperatures in the target plate and rod by 1-D equations, they were calculated with an assumption that the heat deposition rate over the target is uniform at the value obtained by Fig. 2(b). The predicted temperatures are expected to be lower, i.e., have some safety margin comparing with those by the 3-D results due to heat conduction along the plate and the rod.

The thermal hydraulics, material dynamics and neutronics conditions for the safe and high neutronics performance target are as follows:

(a) The heat flux at the target surface is below the critical heat flux.
(b) The temperature at the target surface is below the saturation temperature of water to avoid boiling inception.
(c) The maximum temperature in the target is below a certain temperature much lower than the melting point of the target material.
(d) The thermal stress in the target is below a certain value smaller than the yield stress or the stress which causes the deformation of the coolant channel.
(e) Averaged density of the target is as high as possible for neutron performance.

The conditions of (a) and (b) are based on the heat convection in the coolant and those of (c) and (d) on the heat conduction in the target. The conventional equations are used for thermal hydraulics. The coolant temperature in the channel can be calculated by the enthalpy conservation using the values by Fig. 2(a). The wall surface and the maximum temperatures are mainly discussed in this report. Since the critical heat fluxes for the coolant conditions were reported to be much higher than the heat fluxes estimated by the conditions (b) and (c) by Mishima et al. [2], they are not discussed in this

Table 1
Convectional thermal hydraulics equations

Heat flux and wall temperature
$q = \frac{Qd}{2} = h(T_w - T_L)$
$Nu = 0.023Re^{0.8}Pr^{0.4} \quad Nu = \frac{hd}{\lambda_L} \quad Re = \frac{ud}{\nu_L}$
Maximum temperature
$T_{max} - T_w = -\frac{1}{8\lambda_s}Qd^2$

report. The thermal stress should be discussed for the 3-D configuration (Table 1).

High temperature use of tungsten under irradiation condition is recommended from views of material default recovery and spallation hydrogen movement. Takenaka et al. [3] suggested to increase the tungsten temperature more than 500 °C. It is difficult to increase the tungsten temperature in the cladding plate because it is well thermally contacted to the tantalum cladding by HIP and the cladding is directly cooled by water. Increase of the temperature difference causes serious increase of thermal stress. While, the tungsten rod temperature can be increased by increasing the gap between the rod and the sheath. Therefore, high temperature tungsten design is possible for the rod target when the conditions (a)–(e) are satisfied.

The plate thickness and the rod diameter of the targets allowing the conditions (a)–(d) can be calculated at the heat generation rate distribution. The thickness of the target which agrees with the conditions (a) and

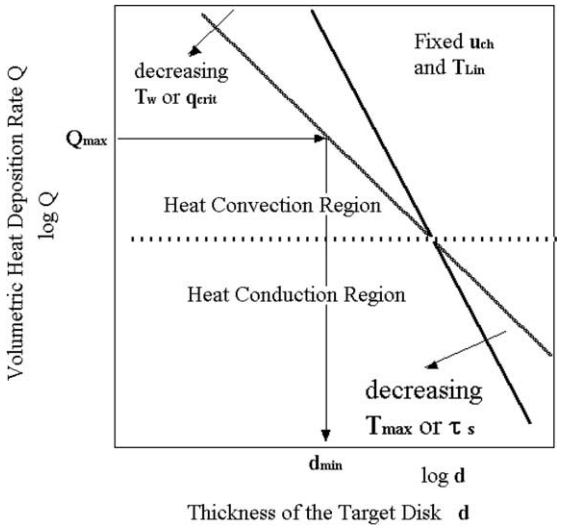

Fig. 4. Schematic diagram for the relations between target plate thickness, d, and volumetric heat deposition rate, Q, d–Q diagram.

(b) is proportional to the heat deposition rate while that with the conditions (c) and (d) proportional to its square. The relation between the heat deposition rate and the thickness of the target plate is illustrated by a d–Q diagram in Fig. 4, [4]. The minimum target thickness, d_{min}, is determined by the maximum heat deposition rate, Q_{max}, as shown in the figure.

Neutrons are generated mainly in the front part of the target and the moderators are placed there. The

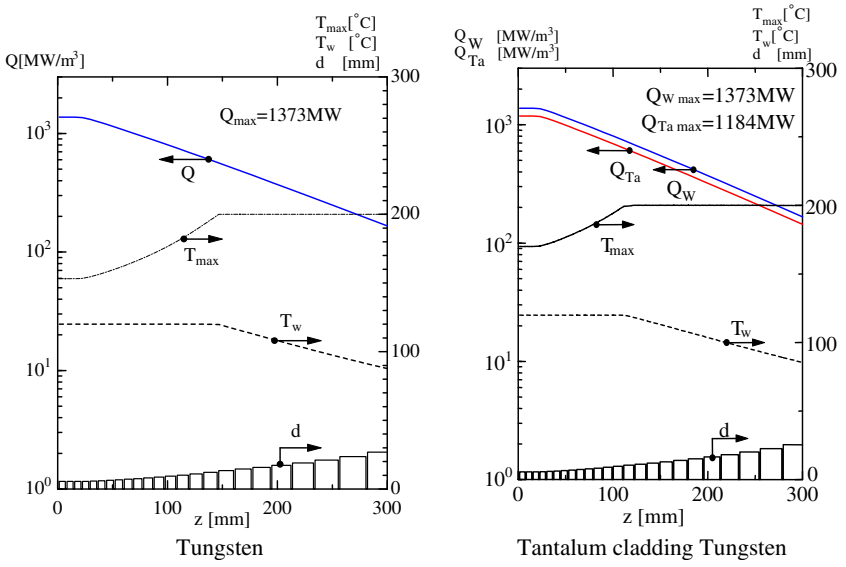

Fig. 5. Plate target design.

effective length of the target L_{eff} is assumed to be 300 mm in the present calculation of the averaged density ρ_{av} from the moderator configuration to discuss on the condition (e).

The limit of the wall temperature can be changed by the coolant pressure and the wall temperature can be decreased when the heat transfer augmentation is applied. The limit of the maximum temperature was determined by the material strength and the target shape. The thickness of the target plates are determined when the limits of the wall temperature, T^*_w, and the maximum temperature, T^*_{max}, are given and the water flow conditions of

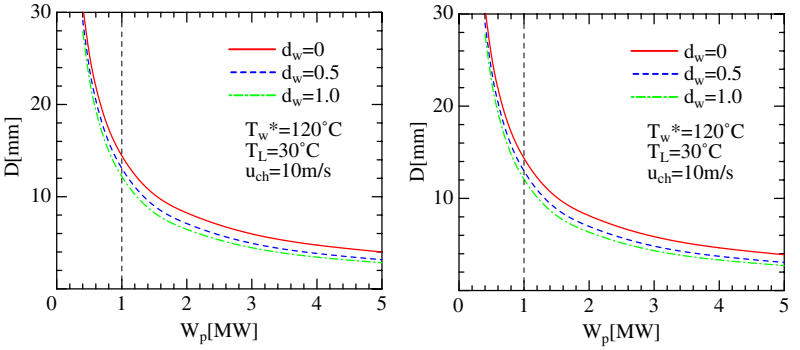

Fig. 6. Rod target design.

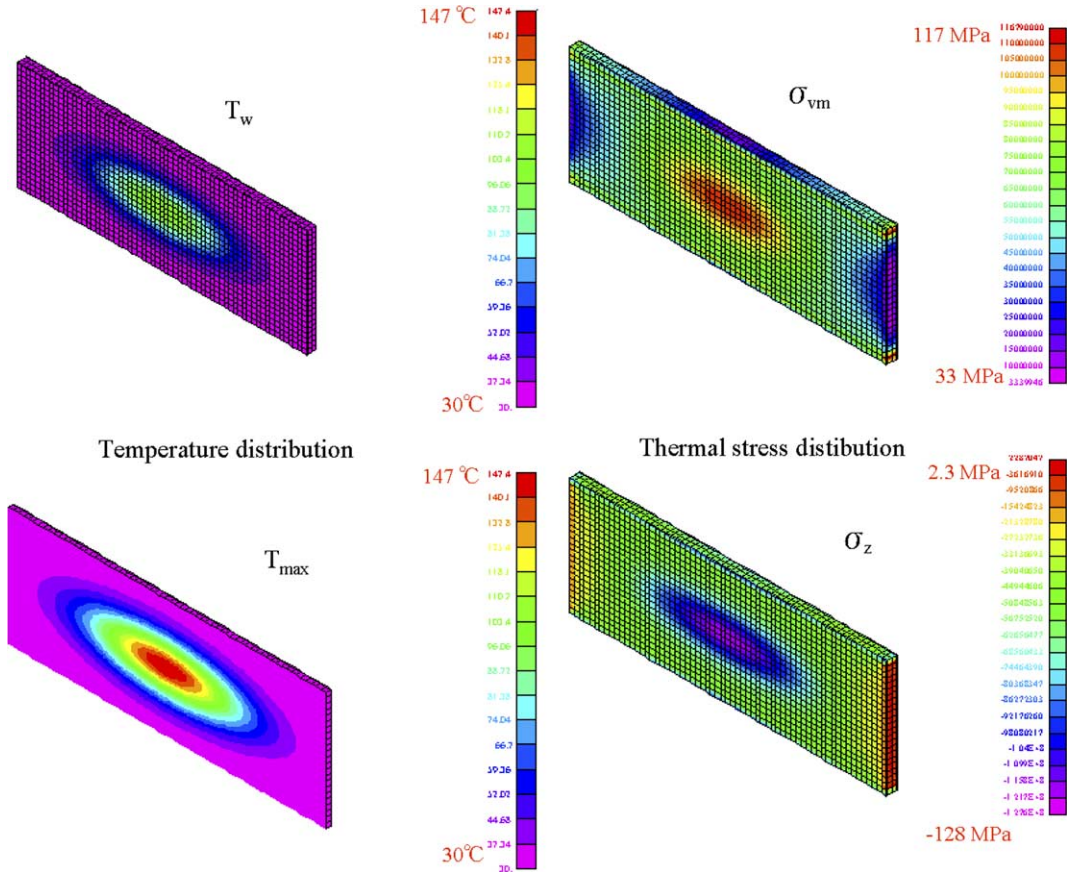

Fig. 7. Temperature and thermal stress distributions in a plate target.

the velocity and inlet temperature are fixed. The minimum thickness d_{min} was determined at the maximum volumetric heat deposition rate, Q_{max}, at first. By placing the plates parallel from the beam window with a gap of 1.5 mm to the maximum point, the plate thicknesses were calculated by the heat deposition rate at the plate position by the distribution in Fig. 2(b) after the maximum point. The thicknesses were calculated in the heat convection region, i.e., determined by T^*_w at first and then in the heat conduction region by T^*_{max} as discussed in the d–Q diagram. The diameter of the rod, D, is determined by the wall temperature limit at the peak of the heat deposition rate.

An example of the designed results for the tungsten and tantalum cladding tungsten plates along the target depth, z, for the beam power, $W_p = 1$ MW, is shown in Fig. 5 on the thickness, d, the wall temperature, T_w, the maximum temperature, T_{max}, the heat flux, q, and the volumetric heat deposition rate, Q, for the water velocity in a channel, $u_{ch} = 10$ m/s, the inlet water temperature, $T_{in} = 30$ °C when the limits of the wall temperature and the maximum temperature are determined as $T^*_w = 120$ °C and $T^*_{max} = 200$ °C, respectively. The minimum thickness of the plate was about 6 mm. If the plate thickness and the wall shear stress are acceptable for the target material, the plate target can be designed by this method. The calculated diameters of the rod target, D, sheathed with Zircaloy and stainless steel for the same conditions as above are plotted in Fig. 6 against the beam power up to 5 MW. The gap between the rods, d_w, is varied 0, 0.5 and 1 mm. The gap can be fixed with spirally wrapping wires as are used in a rod bundle for sodium cooled fast breeder reactors. The wire may augment the heat transfer and the augmentation was considered as the safety margin. The rod bundle without a gap, $d_w = 0$, is not practical but the calculation was made for the comparison. The diameter for 1 MW is around 13 mm similar to the fuel rod diameter of light water nuclear reactors. Leimann et al. [5] reported that clusters were found in Zircaloy sheath of a lead rod target irradiated at SINQ in PSI by neutron radiography. They estimated that the clusters were made from hydrogen generated in the lead rod by the spallation reaction and penetrated into the Zircaloy sheath. Therefore, stainless steel is employed to the rod sheath in the present design.

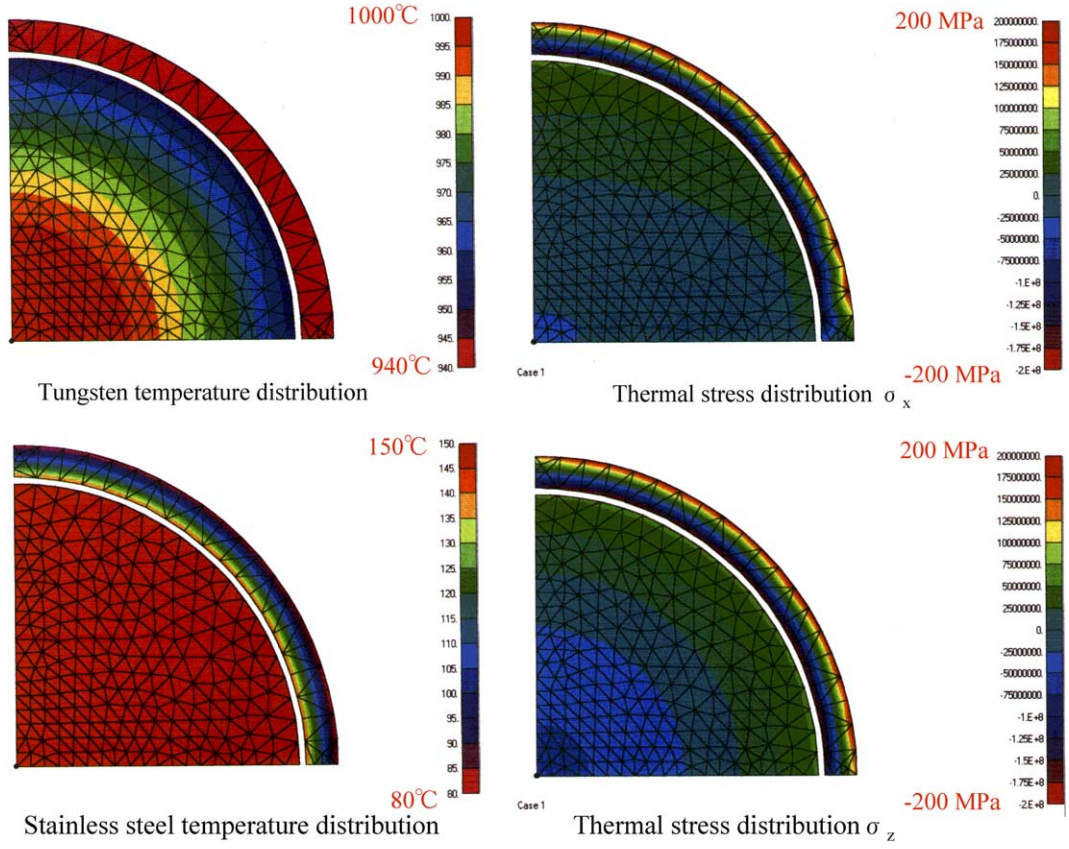

Fig. 8. Temperature and thermal stress distributions in a rod target.

The thermal stress of the targets discussed in 1-D design was calculated in 3-D by a FEM software, NASTRAN. Calculation was carried out at the peak of the heat deposition rate point in Fig. 3. The cross-sectional distribution $Q(x,y)$ [W/m^3] was calculated by the Monte-Carlo method and fitted as

$$Q(x,y) = 1440\exp\left\{-\left(\frac{x^2}{2\times(32.3\times10^{-3})^2} + \frac{y^2}{2\times\left(32.3\times10^{-3}\times2/7\right)^2}\right)\right\}. \quad (1)$$

Examples of the temperature and the thermal stress distributions are shown in Fig. 7 for the tungsten plate 6 mm in thickness and in Fig. 8 for the tungsten rod 9 mm in diameter sheathed by the stainless steel tube 0.5 mm in thickness with 0.1 mm in gap. The temperatures of the tungsten and the stainless steel are much lower than the melting points. The thermal stress is below 200 MPa. Few data have been reported on the material strength of irradiated tungsten. Baker et al. [6] simulated the thermal stress of a tungsten alloy target at LANSCE in the operating condition. Maximum radial tensile stress was about 330 MPa. Maloy et al. [7] reported that compression yield stress of pure tungsten increased by the irradiation up to 23 dpa and higher than 1000 MPa. The strength of irradiated stainless steel is enough for the stress below 200 MPa. It is expected that the design targets can be used safely.

The averaged densities of the targets by the 1-D design are plotted against the beam powers up to 5 MW and are compared with the mercury density of 13.6 g/cm^3 in Fig. 9. The density is higher for the tantalum cladding tungsten plate, Zircaloy sheathed tungsten rod and mercury in order at the beam power less than 1 or 2 MW. The averaged density is low for the solid targets especially low for the rod targets for higher beam power up to 5 MW. It can be seen that solid target is more suitable than mercury liquid target for the beam less than 1 or 2 MW.

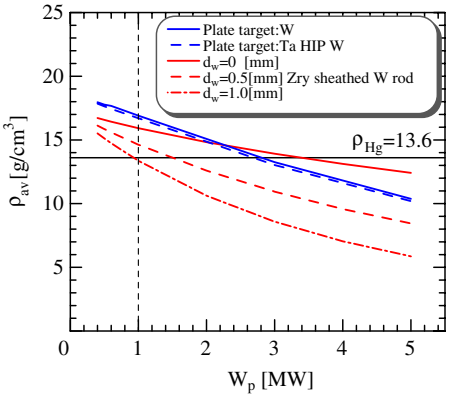

Fig. 9. Comparison of target averaged densities.

3. Decay heat

The decay heat of the solid target is much higher than that of mercury. The decay heat of the tantalum cladding tungsten plate target designed as shown in Fig. 5 was calculated by Kiyanagi et al. in this issue. Some results are reported by using some codes and the maximum values were used to estimate the decay heat removal. A temporal and three-dimensional decay heat rate equation $Q(x,y,z,t)$ [W/m^3] was fitted as

$$Q(x,y,z,t) = Q_{\max}Q(x,y)Q(z)Q(t), \quad (2)$$

where the cross-sectional distribution was

$$Q(x,y) = 5.32\exp\left\{-\left(\frac{x^2}{2\times0.0421^2} + \frac{y^2}{2\times0.0204^2}\right)\right\}, \quad (3)$$

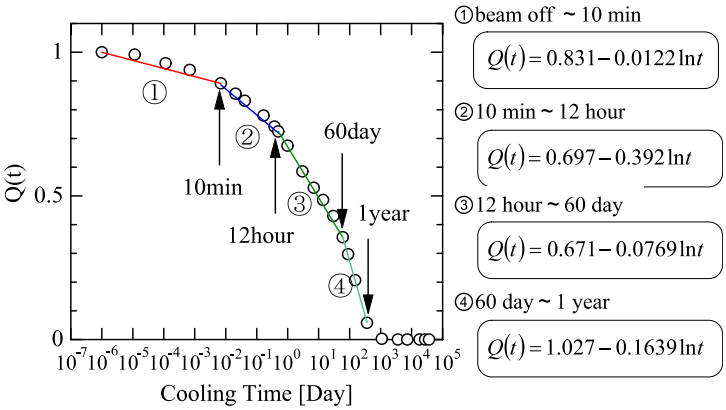

Fig. 10. Time decay fitting.

the axial variation was

$$Q(z) = [1 - \exp\{-(z+11)/10\}]\exp(-z/265) - 1.5\times10^{-6}z^2 + 0.12 \quad (4)$$

and the time decay $Q(t)$ was fitted as shown in Fig. 10.

Fig. 11 shows the total decay heat for the plate targets with and without the tantalum cladding designed as shown in Fig. 5 for 1 MW beam power and 1 year irradiation. The ISIS tantalum target has been

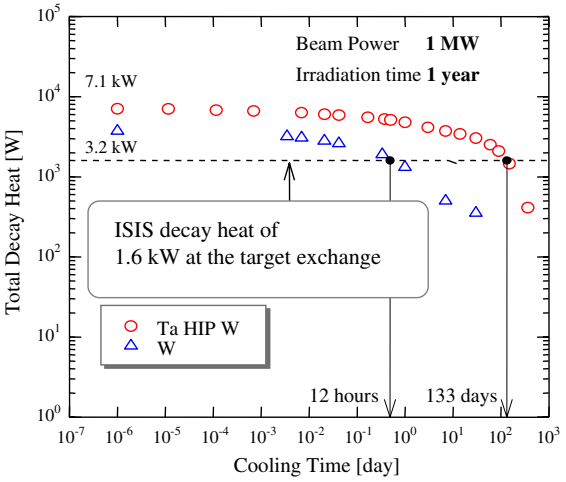

Fig. 11. Total time decay heat of plate targets.

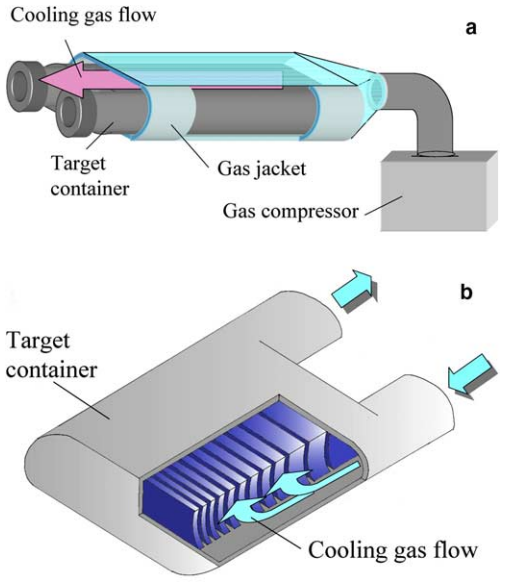

Fig. 12. (a) Decay heat removal by jacket gas cooling from outside of a target container. (b) Decay heat removal gas cooling inside of the target container.

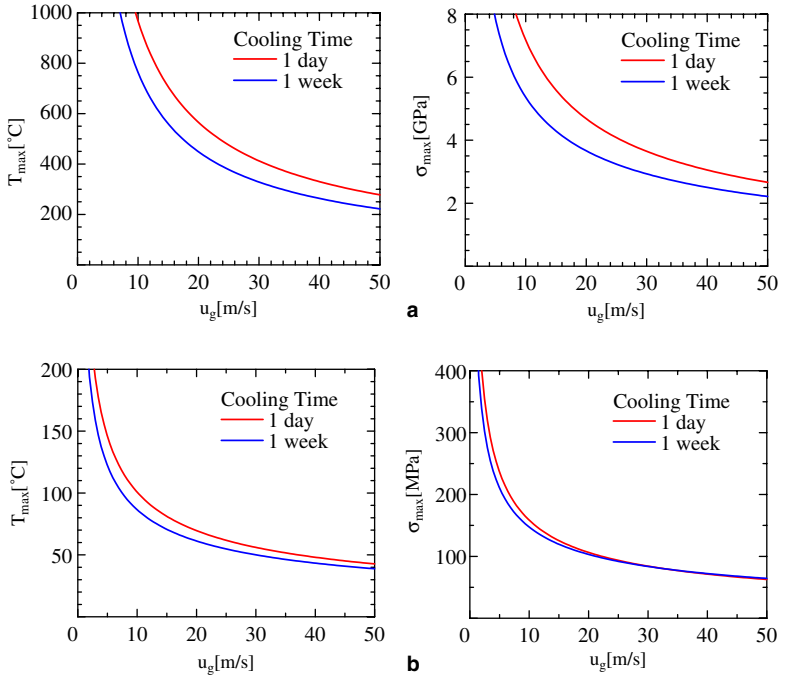

Fig. 13. (a) Designed results of decay heat removal by jacket gas cooling from outside of a target container. (b) Designed results of decay heat removal gas cooling from inside of the target container.

exchanged without cooling after 1 week cooling from beam off. The decay heat of the ISIS target was calculated as 1.6 kW at the target exchange. It is estimated that the target can be exchanged safely without cooling system when the decay heat is below 1.6 kW. The initial decay heat was 3.2 kW without the cladding and decreased rapidly to 1.6 kW in 12 h. However, the initial decay heat with the tantalum cladding was 7.1 kW and it takes more than 100 days to decrease less than 1.6 kW. The long decay time of the cladding target is due to the existence of Ta-182. The cooling for more than 100 days before the target exchange is not practical. The decay heat of the rod targets was not calculated but is estimated to be similar to that of the plate target without the cladding since the decay heat of Zircaloy and stainless steel is very small. Therefore, no special decay heat cooling system is required for the rod target.

Decay heat cooling systems were examined for the tantalum cladding tungsten plate target since the averaged density is the highest and the cladding by the HIP process has already well studied by KAWAI in this issue. Two cooling systems were discussed as shown in Fig. 12(a) and (b). One is the vessel outside cooling using a gas jacket. The target vessel is inserted into a jacket and gas flows between the vessel and the jacket to cool the target outside of the vessel before the water flow stop and drainage. The other is gas cooling inside of the vessel. Gas is injected into the vessel just after the water drainage. Gas is injected into one pipe and is released to atmosphere from the other pipe during the target exchange. Then the exchanged target is put into a water pool. Maximum temperature and thermal stress during the gas cooling by above methods were obtained by the 3-D FEM calculation using the decay heat deposition rate given by Eq. (2) against the gas velocity in Fig. 13(a) and (b). The maximum temperature and thermal stress are high for the gas jacket method even for high gas velocity conditions. The target vessel may be destroyed or disfigured by this cooling method. They are not so high by the method of gas injection inside of the vessel. It is expected that this method is practical though an auxiliary gas pipe-line is required and the safety during the target exchange should be considered.

4. Conclusions

Thermal hydraulic design and decay heat removal of a water cooled solid target for a spallation neutron source were examined based on the neutronics calculations.

1. The averaged density order of the designed target for the beam power less than 1 MW was from highest to lowest: tantalum–clad tungsten plate, sheathed tungsten rods and mercury.
2. The decay heat was high for the tantalum–clad tungsten plate. The gas cooling inside of the target container was required at the target exchange.
3. The stainless steel sheathed tungsten rod target was recommended for the spallation neutron sources beam power less than 1 MW.

References

[1] Y. Kiyanagi, M. Furusaka, in: Proceeding of the Seventh International Conference Nuclear Engineering, Tokyo, Japan, 19–23 April 1999, ICONE-7231.
[2] K. Mishima et al., in: Proceeding of the Fourth Meeting International Collaboration on Advanced Neutron Sources, vol. 1, Utica, USA, 14–19 June 1988, p. 411.
[3] N. Takenaka et al., in: Proceeding of the Fourth Meeting International Collaboration on Advanced Neutron Sources, vol. 1, Utica, USA, 14–19 June 1988, p. 424.
[4] T. Tanabe, private communication.
[5] E. Leimann et al., PSI Ann. Rep. (2002) 35.
[6] G.D. Baker et al., Nucl. Instrum. and Meth. A 359 (1995) 451.
[7] S.A. Maloy et al., Mater. Trans. 43 (4) (2002) 1.